

Hybrid DC–DC Boost Converter for Standalone Photovoltaic Systems

David Etor

Department of Electrical and Computer Engineering
Baze University
Abuja, Nigeria

Abstract— The model of a hybrid dc-dc boost converter, which consists of the conventional and a 2-phase interleaved dc-dc boost converters, is reported. The efficiency of the hybrid converter is well above 90% and remains so throughout the operating period of the system. The model is simple and compact, and will be very useful in applications where a round-the-clock high efficiency performance is of paramount importance.

Keywords— Interleaved dc-dc boost converters, conventional dc-dc boost converters, hybrid dc-dc boost converters, photovoltaic systems, converter efficiency

I. INTRODUCTION

Due to the increasing strict regulations on emissions and concerns about finite fossil fuel supply, global warming and limitations on conventional energy resources, renewable energy sources such as photovoltaic (PV) systems are attracting immense research interest. The PV systems simply convert radiant energy into electrical energy [1]-[5]. The PV systems can be operated as a grid-connected system [6]-[7] – where the power it generates is added to the grid – and as a stand-alone system [4], [8] typically used in rural locations for applications such as lighting, powering of water heaters and pumps etc. When the PV system is operated as a stand-alone system, its efficiency is of paramount importance; and hence, it is vital that maximum power is extracted from the system at all operation times. One of the main drawbacks of the PV system when used for high voltage stand-alone applications is the relatively low output voltage of the individual PV modules. The cost of obtaining the number of PV modules that may be required to generate high values of dc voltage (e.g. 48 volts) is normally high. For this reason, in most cases, a dc-dc power electronic boost converter is incorporated into the system to step-up the output voltage of the PV module or of a few of them to a regulated desired value [9].

The use of the conventional dc-dc boost converter (which comprises “bi” converter) and the interleaved dc-dc boost converter (which comprises “n” number of converters) topologies for the stand-alone PV systems have been reported in the literature [10]-[12]. It was found that the conventional dc-dc boost converter offer better efficiency when the PV module output power is low thus making it more desirable for the stand-alone application under weak light conditions [13], whilst the interleaved dc-dc boost converter offer improved efficiency when the PV output power is high thus making it more desirable for the stand-alone application under strong light conditions [10]-[11]. While it is being debated which among the two converter topologies is more desirable for the

stand-alone PV systems, it is arguable that each of them possess advantages that the other does not possess.

This paper proposes a hybrid dc-dc boost converter topology model, which exploits the advantages of the conventional dc-dc boost converter and the interleaved dc-dc boost converter so that better efficiency can be obtained from the system during all operating times irrespective of the light condition there is.

II. SYSTEM DESCRIPTION

A typical stand-alone system comprises of PV module (or arrays of it), maximum-power-point-tracking (MPPT) device, dc-dc boost converter (for supplying dc loads) and dc-ac converter (for supplying ac loads) as shown in Fig. 1. The PV module converts the solar energy to electrical energy. The maximum power being produced by the PV module is tracked at all times by the MPPT and supplied to the dc-dc boost converter. The dc-dc boost converter then steps up the voltage to a desired value and fed to the dc load. The dc-ac boost converter is used to supply ac loads. This work focuses only on the dc-dc converter.

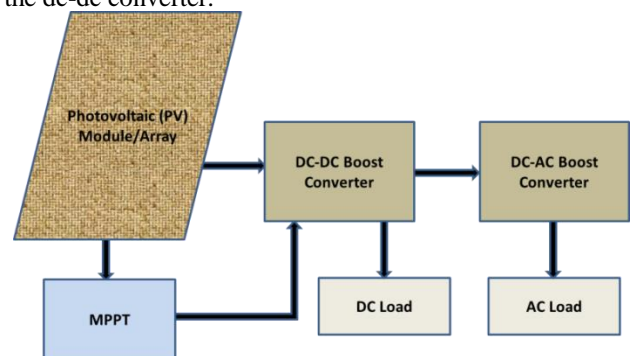


Fig. 1. Typical standalone PV system.

III. MODELLING OF CONVENTIONAL AND INTERLEAVED DC-DC CONVERTERS

The conventional dc-dc boost converter in its basic form as shown in Fig. 2 comprises of an inductor, L , a switch, S , e.g. a MOSFET, a rectifier diode, D , and an output capacitor, C .

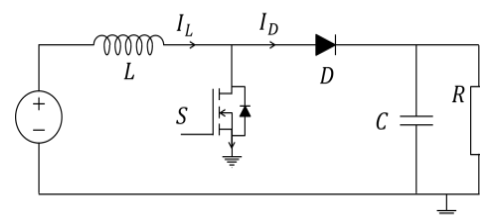


Fig. 2. Basic circuit of a typical conventional dc-dc boost converter.

The conventional dc-dc boost converter is widely used for dc-dc conversion in PV systems [13] due to the simplicity in circuit and system design, moderate voltage stress on its components and high conversion efficiency. In this work, a moderate power dc-dc boost converter with the following specifications was modelled and simulated using Matlab. The parameters for the design are: Minimum input voltage $V_{in(min)} = 15 V$, Maximum input voltage $V_{in(max)} = 19 V$, Desired output voltage $V_{out} = 24 V$, Maximum output current $I_{out(max)} = 0.8 A$, Load resistance $R = 30 \Omega$, Estimated worst case efficiency $\eta = 85\%$, Switching frequency $f_s = 10 kHz$. 10kHz switching frequency was chosen for the design because the converter is a moderate power type, and hence the stress on the components needs to be reasonably minimized. For a lower power type, the switching frequency can be much higher, even into the MHz regime.

The main components values to calculate for in the converter circuit are the inductor and output capacitor values. The inductor value is given by Eqn. 1:

$$L = \frac{RD(1-d^2)}{2f_s} \quad (1)$$

where d is duty cycle, given by:

$$d = 1 - \frac{V_{in(max)} \cdot \eta}{V_{out}} \quad (2)$$

The duty cycle, d , was found to be 0.47, and the inductor values, $L = 549 \mu H$, and was approximated to $L = 560 \mu H$, as that is the nearest standard value that is available in the market. The output capacitor, other than storing and delivering energy, minimizes the converter output voltage ripple, ΔV_{out} . The equivalent series resistance (ESR) inherent in capacitors is therefore preferred to be very small, as it may add further ripple to the output voltage ripple, as shown in Eqn. 4. Hence the main parameters considered when selecting the output capacitor are its capacitance and its ESR. The estimate for the output capacitance, C_{out} , can be calculated by Eqn. 3.

$$C_{out} = \frac{I_{out(max)} \cdot d}{f_s \cdot \Delta V_{out(ESR)}} \quad (3)$$

where $I_{out(max)}$ is the converter maximum output current and;

$$\Delta V_{out(ESR)} = ESR \left(\frac{I_{out(max)}}{1-d} + \frac{\Delta I_L}{2} \right) \quad (4)$$

where $\Delta V_{out(ESR)}$ is the additional output voltage ripple due to capacitors ESR and ΔI_L is the inductor ripple current. The estimate for the inductor ripple current is 20% to 40% of the output current as given by Eqn. 5.

$$\Delta I_L = (0.2 \text{ to } 0.4) I_{out(max)} \cdot \frac{V_{out}}{V_{in}} \quad (5)$$

It was found that $\Delta I_L = 0.512 A$, $\Delta V_{OUT(ESR)} = 0.53 V$, and the estimate for the output capacitance is, $C_{OUT(MIN)} = 70.9 \mu F$. Note that this value is the minimum capacitance from where the capacitance of the output capacitor can be adjusted to a value for a desired output voltage ripple. The capacitance of the output capacitor used for this project is $220 \mu F$.

The interleaved converter comprises of a number of the conventional converters connected in parallel, whereby the converters share the stresses a single converter should, thus minimizing losses due to conduction and switching, and consequently improving the system overall efficiency. As the current and switching frequency stresses are equally shared among each of the multiple converters [10], [11], each of them operates under 1/n of the total operating current and switching frequencies. These presents the following advantages of the topology over the conventional type; reduced input current ripple, reduced switching and conduction losses, better thermal performance and improved efficiency [10], [11]. Furthermore, since all the multiple converter power channels are combined at the output capacitor, the effective ripple frequency is higher than that of a conventional dc-dc boost converter. In this work, a 2-phase (i.e. 2 conventional converters connected in parallel) interleaved converter was used. The inductor value for each of the two converters connected in parallel can be reduced since the current under which each of the converters operates in is half of the current under which the conventional converter operates in. Therefore in this design, the inductor value, $560 \mu H$ for the conventional converter was reduced to $240 \mu H$ for each of the converters used in the interleaved converter. The current sharing among the two paralleled converters has to be accurate to avoid any of them being loaded less or more than the other. There are several current sharing methods available in literature [14], [15]. The method used here is the current-mode-control [15].

A Solkar 37.08W PV module [16] was modelled using Matlab and was used to supply the developed conventional and a 2-phase interleaved dc-dc boost converters as can be

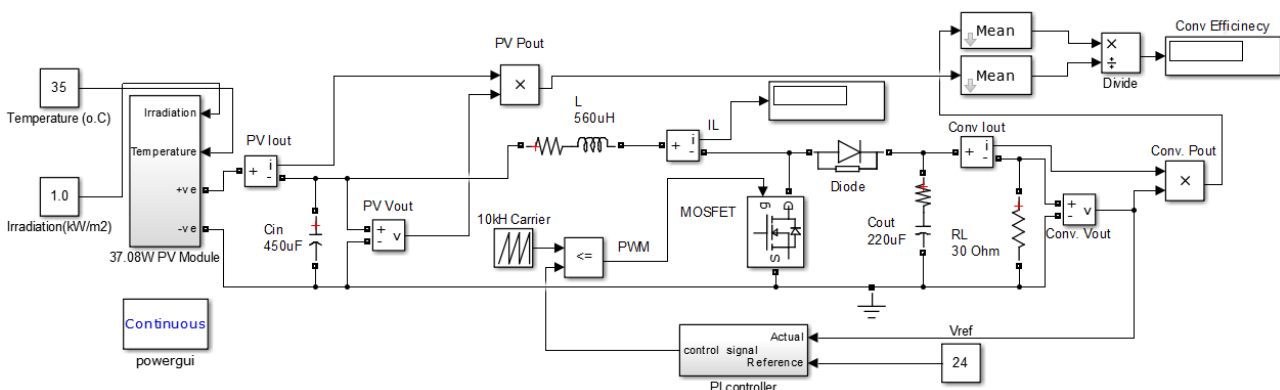


Fig. 3. Model of the standalone PV system using the conventional dc-dc boost converter topology.

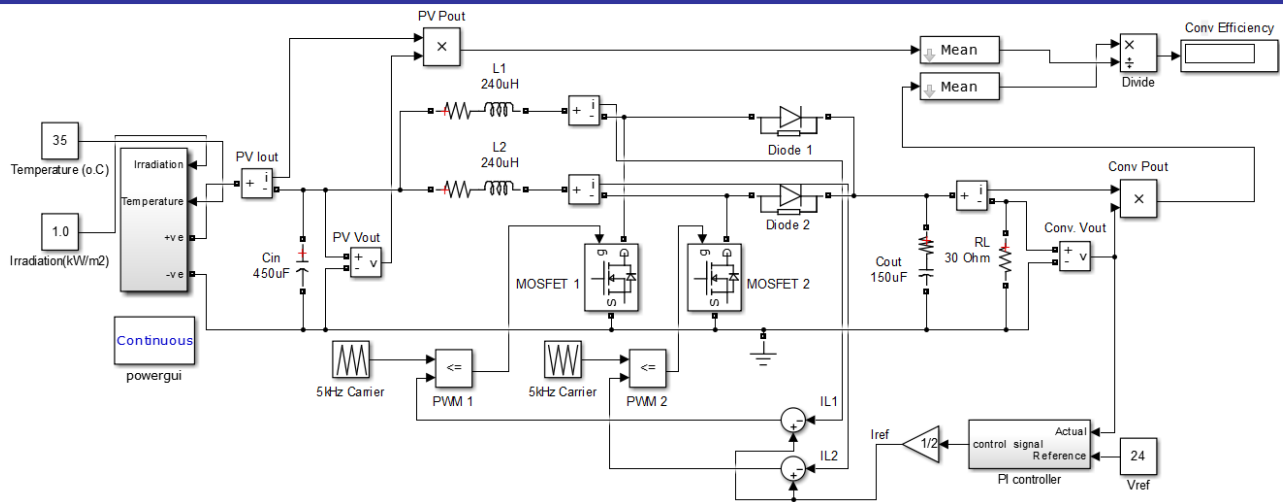


Fig. 4. Model of the standalone PV system using the 2-phase interleaved dc-dc boost converter topology.

seen in Fig. 3 and Fig. 4 respectively.

IV. RESULTS AND DISCUSSIONS

The efficiency of the two converter topologies are compared as the PV output power changes. It is assumed throughout the simulations that the PV operating temperature is constant at 35°C. As irradiation fluctuates, the PV output power also fluctuates. The conventional and interleaved converter topologies respond differently to these fluctuations. Fig. 5 shows the efficiency of the conventional and interleaved dc-dc boost converter models as a function of PV output power.

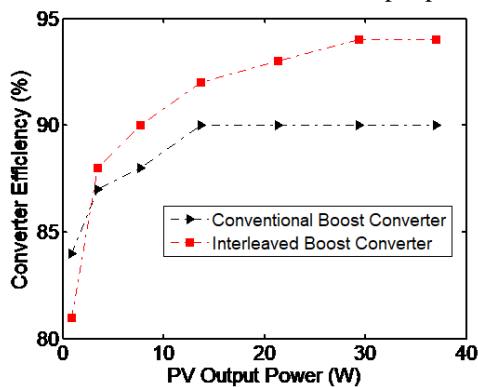


Fig. 5. Efficiency of the conventional and interleaved dc-dc boost converter models vs PV output power.

It can be seen that at low PV output power, the efficiency of the conventional boost converter is higher than that of the interleaved converter. But as the PV output power increases, the efficiency of the interleaved converter becomes higher. This is expected, as, when PV output power is high, losses in the converters become high and hence a decrease in their efficiency. However, the efficiency of the interleaved converter is higher at high PV output power because the losses occurring in the converter are considerably lower due to the sharing of conduction and switching stresses among the multiple converters it consists of.

Since on average, a PV system produces between 30% and 100% of its rated power 80% of its operating time [17], it then means that, generally, in order to maximize the efficiency of the system throughout its operating conditions (i.e. with weak and strong light conditions), considering the results shown in Fig. 5, the advantages the conventional and interleaved dc-dc boost converter topologies presents will have to be exploited. Fig. 6 shows the PV system wherein the two converter topologies are combined and referred to as a hybrid PV system, such that at low irradiation, the conventional converter operates, and at high irradiation, it is disengaged and the interleaved converter operates.

The Ppv subsystem in Fig. 6 contains two identical outputs for the 37.08W Solkar PV module, with a change-over-switch to switch the outputs between the two converter topologies

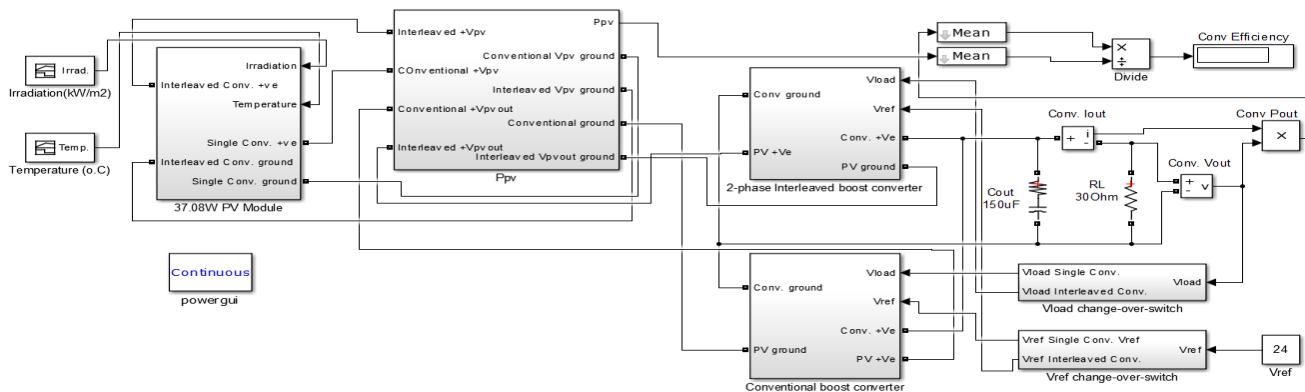


Fig. 6. Model of hybrid dc-dc boost converter.

when required. The two identical outputs were modelled in order to allow for the demonstration of the idea through simulation but in reality, the PV has only one output.

In this simulation, the conventional boost converter is set to operate at the minimum irradiation up to 800W/m^2 , while the interleaved boost converter is set to operate when the PV module is operating at irradiation of 800W/m^2 to 1000W/m^2 . The switching between the operations of two converters is done by the V_{load} and V_{ref} change-over-switch subsystems in Fig. 6. The change-over-switches contains timer-switching schemes, which allows for one of the converters to operate over a predefined time period, and then switches on or off. In this work, the PV system was first set to operate under the irradiation of 800W/m^2 and to supply the conventional boost converter only, from 0 to 0.7 sec of the 1 sec duration for which it was simulated, as shown in Fig. 7(a). During this period, only the conventional boost converter operates. From 0.7 to 1 sec, the system operates under irradiation of above 800W/m^2 and supplies power to the interleaved boost converter only (see Fig. 7(b)). During this time, the conventional boost converter is disengaged completely, with the interleaved boost converter now operating.

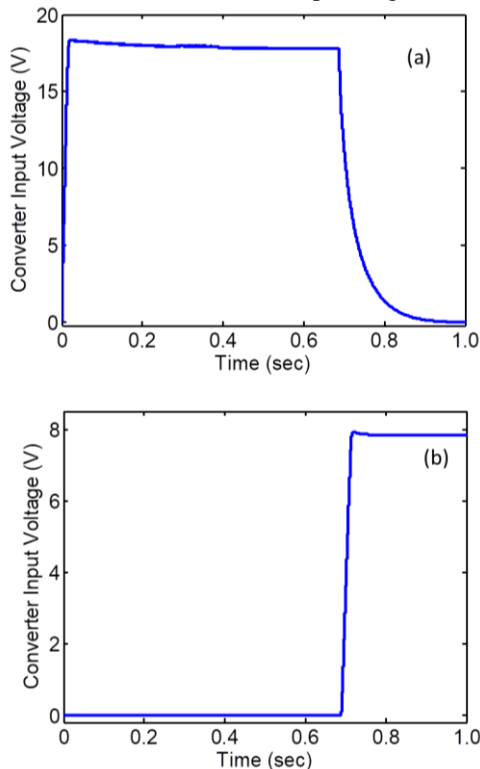


Fig. 7. (a) Input voltage to conventional boost converter from 0 to 0.7 sec., and (b) input voltage to interleaved boost converter from 0.7 to 1 sec.

The timer-switching scheme was developed only for the purpose of simulation. In reality, the system would consist of sensors, which will sense the PV output power, and prompt the switches appropriately. The V_{ref} switching scheme operates exactly as that for V_{load} . The only difference is that V_{ref} supplies reference voltage to the boost converters while V_{load} supplies feedback to the boost converters. The hybrid PV system output voltage is shown in Fig. 8(a), with the system efficiency (in Fig. 8(b)) being over 90% throughout the system operating time.

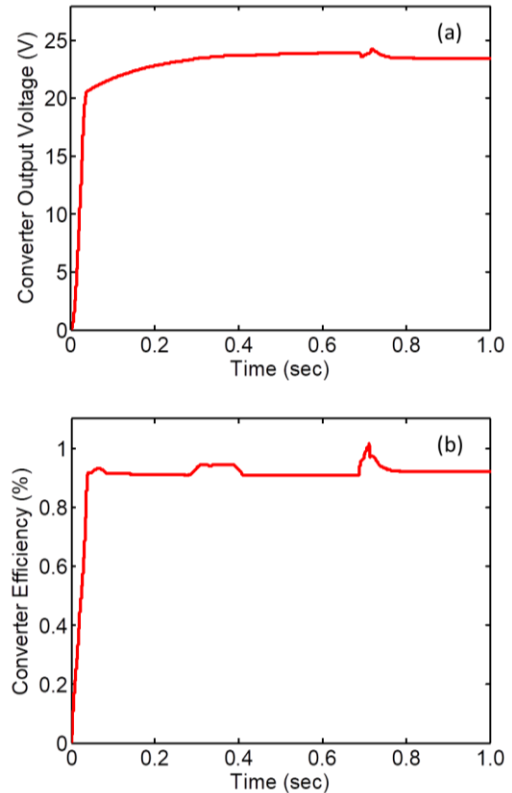


Fig. 8. (a) Hybrid boost converter output voltage, and (b) converter efficiency.

The spike seen in the efficiency around 0.7 sec in Fig. 8(b) is due to the change-over of input voltage from the conventional to the interleaved converter.

V. CONCLUSION

A hybrid dc-dc boost converter, which consists of the conventional and interleaved dc-dc boost converters have been modelled and simulated. The efficiency of the hybrid converter is well above 90% and remains so throughout the operating period of the system. As the proposed converter consists of the conventional and interleaved dc-dc boost converters, the efficiency will be the maximum (well above 85%) irrespective of light conditions. The hybrid dc-dc boost converter comes handy in applications, such as aerospace, where high efficiency is essential at all times.

REFERENCES

- [1] A. D. Bagul, Z. M. Salameh, and B. Borowy, "Sizing of a stand-alone hybrid wind-photovoltaic system using a three-event probability density approximation," *Solar Energy*, Vol. 56, Issue 4, pp. 323-335, April, 1996.
- [2] L. Keller, and P. Affolter, "Optimizing the panel area of a photovoltaic system in relation to the static inverter-Practical results," *Solar Energy*, Vol. 55, Issue 1, pp. 1-7, July, 1995.
- [3] M. Kolhe, S. Kolhe, and J. C. Joshi, "Economic viability of stand-alone solar photovoltaic system in comparison with diesel-powered system for India," *Energy Economics*, Vol. 24, Issue 2, pp. 155-165, March, 2002.
- [4] W. X. Shen, "Optimally sizing of solar array and battery in a standalone photovoltaic system in Malaysia," *Renewable Energy*, Vol. 34, Issue 1, pp. 348-352, January, 2009.
- [5] H. N. Post, and M. G. Thomas, "Photovoltaic systems for current and future applications," *Solar Energy*, Vol. 41, Issue 5, pp. 465-473, 1998.

- [6] S. B. Kjaer, J. K. Pedersen, and F. Blaabjerg, "A review of single-phase grid-connected inverters for photovoltaic modules," *IEEE Trans. Ind. Appl.*, Vol. 41, Issue 5, pp. 1292-1306, October, 2005.
- [7] M. A. Eltawil, and Z. Zhao, "Grid-connected photovoltaic power systems: Technical and potential problems-A review," *Renewable Sustainable Energy Rev.*, Vol. 14, Issue 1, pp. 112-129, January, 2010.
- [8] T. Khatib, A. Mohamed, K. Sopian, and M. Mahmoud, "A New Approach for Optimal Sizing of Standalone Photovoltaic Systems," *Intl. J. Photoenergy*, Vol. 2012, ID 391213, pp. 1-7, 2012.
- [9] V. Salas, E. Olías, A. Barrado, and A. Lázaro, "Review of the maximum power point tracking algorithms for stand-alone photovoltaic systems," *Solar Energy Mat. Solar Cells*, Vol. 90, Issue 11, pp. 1555-1578, July, 2006.
- [10] G. A. L. Henn, R. N. A. L. Silva, P. P. Praça, L. H. S. C. Barreto, and D. S. Oliveira, "Interleaved-Boost Converter With High Voltage Gain," *IEEE Trans. Power Electron.*, Vol. 25, Issue 11, pp. 2753-2761, November, 2010.
- [11] G. Yao, A. Chen, and X. He, "Soft Switching Circuit for Interleaved Boost Converters," *IEEE Trans. Power Electron.*, Vol. 22, Issue 1, pp. 80-86, January, 2007.
- [12] J. L. Santos, F. Antunes, A. Chehab, and C. Cruz, "A maximum power point tracker for PV systems using a high performance boost converter," *Solar Energy*, Vol. 80, Issue 7, pp. 772-778, July, 2006.
- [13] M. A. Farahat, H. M. B. Metwally, and A. E. Mohamed, "Optimal choice and design of different topologies of DC-DC converter used in PV systems, at different climatic conditions in Egypt," *Renewable Energy*, Vol. 43, pp. 393-402, July, 2012.
- [14] B. S. Min, N. J. Park, and D. S. Hyun, "A Novel Current Sharing Technique for Interleaved Boost Converter," *IEEE Power Electronics Specialists Conf.*, Orlando FL, USA, 17-21 June 2007.
- [15] R. P. Singh, and A. M. Khambadkone, "Current Sharing and Sensing in N-paralleled Converters using Single Current Sensor," *IEEE Trans. Ind. Appl.*, Vol. 46, pp. 1212-1214, June, 2010.
- [16] N. Pandiarajan, and R. Muthu "Mathematical Modeling of Photovoltaic Module with Simulink," *Int. Conf. Elect. Energy Syst.*, January, 2011, pp. 314-319.
- [17] A. Berasategi, C. Cabal, C. Alonso, and B. Estibals. "European efficiency improvement in photovoltaic applications by means of parallel connection of power converters", 13th European Conf. Power Electron. Appl., October, 2009, Barcelona, Spain.